

Predictive relationships for seismically induced slope displacements using numerical analysis results

S. D. Fotopoulou¹  · K. D. Pitilakis¹

Received: 11 October 2014 / Accepted: 19 April 2015 / Published online: 26 April 2015
© Springer Science+Business Media Dordrecht 2015

Abstract The aim of the paper is threefold: first, to evaluate earthquake-induced slope displacements using numerical dynamic analysis considering different real acceleration time histories as input motion and varying the resistance and the compliance of the sliding mass; then, to assess the reliability of the numerical approach by comparing the numerically calculated seismically induced slope displacements with predictions using available empirical models and finally, based on the numerical analysis results, to propose new displacement predictive models applicable in earthquake engineering practice, which relate the co-seismic slope displacement with the best correlated intensity parameters. Linear regression analyses are performed to correlate the computed displacements with various intensity measures (IMs). Optimal scalar and vector IMs are identified in a rigorous way based on proficiency (i.e. a composite measure of efficiency and practicality) and sufficiency criteria. The correlation coefficient between the IMs is also considered for the selection of appropriate vector IMs. Both scalar and vector regression analytical predictive expressions are proposed appropriate for probabilistic or deterministic evaluation of the co-seismic permanent slope displacements in regional and local scale. A generic example proves the reliability of the proposed analytical expressions.

Keywords Seismically induced slope displacement · Numerical parametric analysis · Optimal IMs · Displacement predictive models

✉ S. D. Fotopoulou
sfotopou@civil.auth.gr
K. D. Pitilakis
kpitilak@civil.auth.gr

¹ Research Unit of Geotechnical Earthquake Engineering and Soil Dynamics, Department of Civil Engineering, Aristotle University, Thessaloniki, Greece

1 Introduction

It is common practice in geotechnical earthquake engineering to assess the expected seismic performance of slopes and earth structures by estimating the seismically induced permanent ground displacements using one of the available displacement based procedures. Considering that the magnitude of seismic displacements ultimately governs the performance of a slope after an earthquake, the use of such approaches is generally recommended. Typically, two different approaches of increased complexity are proposed to assess permanent ground displacements in case of seismically triggered slides: Newmark-type displacement methods and advanced stress–strain dynamic methods. Newmark-type methods are based on the sliding block assumption first proposed by Newmark (1965) providing an index of the dynamic slope performance. Advanced stress-deformation analyses based on continuum mechanics (finite element, FE, finite difference, FDM) or discontinuum formulations usually incorporating complicated constitutive models, are recently becoming attractive, as they can provide approximate solutions to problems which otherwise cannot be solved by conventional methods e.g. the complex geometry including topographic and basin effects, material anisotropy and non-linear behavior under seismic loading, in situ stresses, pore water pressure built-up, progressive failure of slopes due to strain localization.

The input motion characteristics (i.e. amplitude/intensity, frequency content and duration) comprise the primary contributing factor in the calculation of the amount of earthquake induced slope displacement. Various simplified approaches use single parameters characterizing the ground motion intensity (e.g. peak ground acceleration PGA), the frequency content (e.g. mean period T_m) and the duration (e.g. significant duration D_{5-95}). It has been shown that ground motion intensity has the greatest impact on the displacement prediction while features related to the frequency content and duration display weak correlation with slope displacement (e.g. Saygili and Rathje 2008; Strenk and Wartman 2013). A possible explanation for this could be that the ground motion intensity predicts the onset of slope movement and thus is initially more important than any frequency content or duration parameter in assessing earthquake induced slope displacement (Saygili and Rathje 2008). However, intensity ground motion parameters are usually supplemented by additional parameters characterizing either the intensity or the frequency content and duration of the earthquake ground motion, in order to provide more efficient and sufficient estimates of the seismically induced slope displacements (Bray 2007).

The slope properties associated with the slope geometry, soil strength and stiffness characteristics also play a crucial role in the seismic displacement prediction. In the displacement based approaches, a single parameter, i.e. the yield acceleration coefficient, k_y , is commonly used to represent the overall resistance of the slope. The yield acceleration coefficient depends primarily on the slope geometry and strength of the material along the critical sliding surface and it may be determined through a pseudostatic analysis or by a simplified empirical relationship (e.g. Bray 2007). Low k_y values (near zero) are indicative of a weak slope whereas as k_y increases the strength of the slope increases as well. The stiffness of the slope can be represented by the initial fundamental period of the slope, T_s . For a stiff, nearly rigid slope case T_s approaches zero while for a deformable slope T_s can normally be estimated using a simple analytical expression depending on the shape and the dynamic response characteristics of the potential sliding mass.

Based on these general considerations, the aim of this study is threefold: (a) to assess earthquake induced slope displacements using numerical dynamic analysis by performing a comprehensive parametric study for different slope geometries, soil properties and input

motions; (b) to compare the numerical results in terms of co-seismic permanent slope displacements with available and widely used empirical displacement based models and (c) based on the numerical results, to propose new displacement predictive models applicable in earthquake engineering practice, which relate the co-seismic slope displacement with the best correlated parameters characterizing the intensity of the strong ground motion.

The computed numerical displacements are first compared with the displacements predicted from different empirical Newmark-type displacement procedures. The aim of this comparison is, on the one hand, to gain confidence on the results of the numerical analysis and, on the other hand, to assess the predictive capability of the different displacement based approaches with respect to the more sophisticated numerical analysis.

Linear regression analyses are performed on the numerical analysis results to correlate the computed displacements with various intensity measures (IMs). Optimal scalar and vector IMs are identified in a rigorous way based on proficiency (i.e. a composite measure of efficiency and practicality) and sufficiency criteria. An additional factor, namely the correlation coefficient between the IMs, is also considered for the selection of appropriate vector IMs. Finally, both scalar and vector regression analytical predictive expressions are developed to assess the co-seismic permanent slope displacement. Such expressions may be effectively used in engineering practice within a deterministic or probabilistic framework for the evaluation of the seismic slope displacement both in regional or local scale. At the end a typical example is presented where the co-seismic permanent slope displacements have been estimated using the proposed analytical expressions in comparison with some of the most frequently used ones.

2 Empirical displacement based predictive models

Starting from the pioneer study of Newmark (1965), several empirical models are currently available to predict seismically induced displacements of sliding masses. These generally differ with respect to the assumptions and idealizations used to model the mechanism of earthquake-induced displacement. They are intended for soil slopes that do not undergo significant strength loss (i.e. liquefaction or flow slides). They are grouped into three main types (Jibson 2011): rigid-block, decoupled, and coupled slopes. The rigid-block model originally proposed by Newmark (1965) treats the potential landslide block as a rigid mass (no internal deformation) that slides in a perfectly plastic manner on an inclined plane. The original Newmark rigid sliding block assumption is employed in many of the available simplified slope displacement procedures (e.g. Sarma 1975; Lin and Whitman 1986; Ambraseys and Menu 1988; Yegian et al. 1991; Jibson 2007; Saygili and Rathje 2008 etc.). A quantitative comparison of existing simplified rigid block methods was performed by Cai and Barthurst (1996). Rigid-block analysis is appropriate for analyzing thin, “stiff” landslides but yields quite unconservative results for deep, “flexible” slopes. The dynamic site response and the sliding block displacements are computed separately in the ‘decoupled’ approach (e.g. Makdisi and Seed 1978; Bray and Rathje 1998; Rathje and Antonakos 2011) or simultaneously in the ‘coupled’ stick–slip analysis (Rathje and Bray 2000; Bray and Travararou 2007). Some of the most commonly applicable seismic displacement procedures that account for the soil deformability (both coupled and decoupled) are discussed in Bray (2007). Generally, irrespective of their assumptions to analyze the dynamic slope response, recent approaches (e.g. Watson-Lamprey and Abrahamson 2006; Jibson 2007; Saygili and Rathje 2008; Bray and Travararou 2007; Rathje and Antonakos 2011)

involve larger ground motion datasets and robust mathematical regression techniques and therefore they are expected to yield more reliable estimates of the slope displacement. In the following, four empirical predictive models, namely the conventional analytical Newmark rigid block model (Newmark 1965), the Jibson (2007) rigid block model, the Rathje and Antonakos (2011) decoupled sliding block model and finally the Bray and Travarasou (2007) coupled stick–slip sliding block model, are briefly discussed.

The Newmark conventional analytical rigid block method is used to predict average slope displacements obtained by integrating twice with respect to time the parts of an earthquake acceleration-time history that exceed the critical or yield acceleration, a_c ($k_y \cdot g$) (i.e. threshold acceleration required to overcome shear soil resistance and initiate sliding). The second approach is a simplified rigid block model proposed by Jibson (2007), which predicts slope displacement as a function of Arias intensity (I_a) and critical acceleration ratio (a_c/PGA). This method was selected considering that Arias intensity was found to be the most efficient IM for stiff, weak slopes (Travarasou 2003). The third method is a two-parameter vector (PGA, PGV) model proposed by Rathje and Antonakos (2011). This model is often recommended for use in practice due to its ability to significantly reduce the variability in the displacement prediction (Saygili and Rathje 2008). For flexible sliding, k_{max} (e.g. peak value of the average acceleration time history within the sliding mass) is used in lieu of PGA and $k\text{-vel}_{max}$ (e.g. peak value of the $k\text{-vel}$ time history provided by numerical integration of the $k\text{-time}$ history) is used to replace PGV. The last one is the Bray and Travarasou (2007) model. In this model cumulative displacements are calculated using the nonlinear fully coupled stick–slip deformable sliding block model proposed by Rathje and Bray (2000) to capture the dynamic response of the sliding mass. They use a single intensity parameter to characterize the equivalent seismic loading on the sliding mass, i.e. the ground motion's spectral acceleration S_a at a degraded period equal to $1.5T_s$, which was found to be the optimal one in terms of efficiency and sufficiency (Bray 2007).

It is noted that Newmark method is an analytical rigid block approach whereas Jibson (2007), Rathje and Antonakos (2011) and Bray and Travarasou (2007) models are essentially regression models of the analytical form of the rigid-block, decoupled and coupled methods respectively. As such, Newmark analytical method uses the entire time history to characterize the seismic loading as opposed to the simplified methods of Jibson (2007), Bray and Travarasou (2007) and Rathje and Antonakos (2011) that use one [I_a , $S_a(1.5T_s)$] and two (PGA, PGV) intensity parameters respectively. In this way, uncertainties (and potential biases) associated to the selection of the ground motion intensity parameters are limited in the Newmark conventional analytical approach.

Table 1 summarizes the functional form of the three simplified sliding block models examined in this study. The herein models yield mean (Jibson 2007) or median (Rathje and Antonakos 2011, Bray and Travarasou 2007) values of seismic slope displacement when the standard deviation (the last term in the equations) is ignored. These median or mean displacement values are used in this study for the comparison with the herein calculated numerical displacements.

3 Numerical parametric analysis

Two dimensional (2D) fully non-linear numerical analyses are performed for idealized step-like slope configurations applying the finite difference code FLAC2D (Itasca 2011) considering different real acceleration time histories as input motion and varying the

Table 1 Functional form of the simplified sliding block models used in this study

Model	Functional form
Jibson (2007) simplified rigid block model	$\log(D) = 0.561 \log(I_a) - 3.833 \log(a_c/PGA) - 1.474 \pm \sigma$ where D is in cm, I_a in m/s and PGA and a_c in g
Rathje and Antonakos (2011) simplified decoupled sliding block model	For rigid sliding masses $\ln(D) = -1.56 - 4.58 \left(\frac{k_y}{PGA}\right) - 20.84 \left(\frac{k_y}{PGA}\right)^2 + 44.75 \left(\frac{k_y}{PGA}\right)^3 - 30.50 \left(\frac{k_y}{PGA}\right)^4 +$ $- 0.64 \ln(PGA) + 1.55 \ln(PGV) + \varepsilon \sigma_{inD}$ where D is in cm, PGA in g and PGV in cm/s For flexible sliding masses, k_{max} (in g) and $k\text{-vel}_{max}$ (in cm/s) are used to replace PGA and PGV respectively and a term conditioned to T_s is added: $\ln(D_{flexible}) = \ln(D_{PGA,PGV}) + 1.42T_s \quad \text{for } T_s \leq 0.5$ $\ln(D_{flexible}) = \ln(D_{PGA,PGV}) + 0.71 \quad \text{for } T_s > 0.5$ where $D_{flexible}$ is in cm and T_s in seconds
Bray and Travarasrou (2007) simplified coupled stick–slip sliding block model	For the flexible sliding block case ($T_s > 0.05$): $\ln(D) = -1.10 - 2.83 \ln(k_y) - 0.333 (\ln(k_y))^2 + 0.566 \ln(k_y) \ln(S_a(1.5T_s))$ $+ 3.04 \ln(S_a(1.5T_s)) - 0.244 (\ln(S_a(1.5T_s)))^2 + 1.50T_s + 0.278 (M - 7) \pm \varepsilon$ where D is in cm, T_s in seconds and $S_a(1.5T_s)$ in g For the nearly rigid sliding block case ($T_s < 0.05$): $\ln(D) = -0.22 - 2.83 \ln(k_y) - 0.333 (\ln(k_y))^2 + 0.566 \ln(PGA)$ $+ 3.04 \ln(PGA) - 0.244 (\ln(PGA))^2 + 1.50T_s + 0.278 (M - 7) \pm \varepsilon$ where D is in cm, T_s in seconds and PGA in g

resistance and the compliance of the sliding mass (characterized by the yield coefficient, k_y , and the fundamental period of the sliding mass, T_s , respectively). In particular, 12 typical 2D stress–strain slope soil models are analyzed with varying geometrical characteristics, material properties of the surface layer as well as strength and stiffness of the potential sliding surface. Figure 1 describes the layout of the problem under study whereas Table 2 summarizes the analyzed models.

A sensitivity analysis is conducted to assure that the boundaries of the considered soil models are far away enough to avoid rebounding (e.g. Morales-Esteban et al. 2015). Thus, models m1–m4 have a total length of 400 m and a thickness of the elastic bedrock equal to 30 m, models m10 and m12 a total length of 900 m and a thickness of the elastic bedrock equal to 30 m while for the rest models (m5–m9 and m11) the total length and the thickness of the elastic bedrock increase to 1200 and 70 m respectively. The thickness of the stiff clayey soil layer is considered equal to 30 m for all analyzed models.

The discretization allows for a maximum frequency of 10 Hz to propagate through the grid without distortion. A finer discretization is adopted in the slope area with quadratic elements of 0.5–1.5 m × 0.5–1.5 m, whereas towards the boundaries of the model the mesh is coarser (1.5–2.5 m × 1.5–5 m). It is noted that the element size varies for the different analyzed soil models depending on the stiffness of each layer (it increases for the stiffer deeper layers). In total, approximately 9500 quadrilateral elements are considered for models m1–m4, 18,500 elements for models m10 and m12 and 21,000 elements for the rest analyzed models (m5–m9 and m11). Free field absorbing boundaries (Cundall et al. 1980) are applied along the lateral boundaries whereas quiet boundaries (Lysmer and Kuhlemeyer 1969) are applied along the bottom of the dynamic model to further reduce the

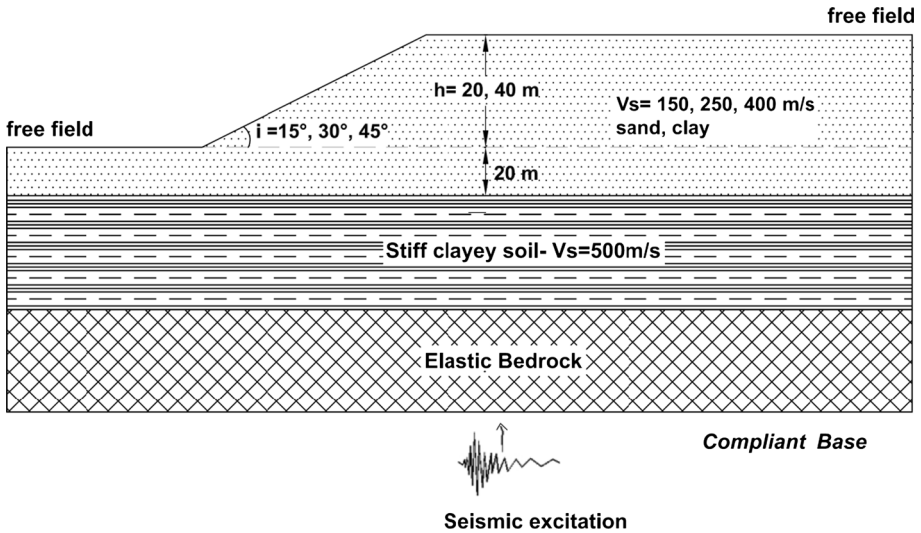


Fig. 1 Layout of the problem under study

effect of trapped energy and artificially reflected waves. The soil materials are modeled using Mohr–Coulomb elastoplastic constitutive model characterized by its yield function and flow rule (Itasca 2011). The failure envelope corresponds to the Mohr–Coulomb criterion (shear yield) with tension cutoff (tension yield function) assuming a nonassociated flow rule for shear failure, and an associated rule for tension failure. Thus, when irreversible strain accumulation takes place the energy dissipation is intended to be captured through the yield model. A small amount of mass and stiffness-proportional Rayleigh damping (3 % for the soil materials and 0.5 % for the elastic bedrock) is also assigned to account for the energy dissipation during the elastic part of the cyclic response. The center (minimum) frequency of the Rayleigh damping (f_{\min}) is selected to lie between the natural modes of the models, f_1 (defined by the downhill and uphill resonant frequencies respectively) and $f_2 = 5 \cdot f_1$ based on common practice (e.g. Kwok et al. 2007). This range includes the models' natural frequencies and the predominant frequencies of the input motions.

Generic soil properties are considered based on the available literature and engineering judgment. These are selected to vary for the surface layer while they are kept constant for the intermediate layer and the elastic bedrock. The mechanical properties adopted for the soil materials and the elastic bedrock are presented in Table 3.

The initial fundamental period of the sliding mass (T_s) is estimated using the simplified expression: $T_s = 4H/V_s$, where H is the depth and V_s is the shear wave velocity of the potential sliding mass. The depth of the sliding surface as well as the horizontal yield coefficient, k_y , are evaluated by means of pseudostatic slope stability analyses utilizing the Bishop's simplified method for the critical sliding surface. It's worth noticing that a fixed value of k_y is calculated assuming that no significant strength loss is anticipated in the slope soil material (e.g. no liquefaction or strain softening).

The dynamic input motion consists of SV waves vertically propagating from the base. The seismic input applied along the base of the dynamic model consists of a set of 40 real acceleration time histories recorded on rock outcrop or very stiff soil (soil classes A and B according to EC8) and derived from the SHARE database (Seismic Hazard Harmonization

Table 2 Analyzed models

Yield coefficient k_y	Slope height h (m)	Slope inclination i (°)	Soil properties of the surface layer (see Table 3 for details)	Depth of the sliding mass H (m)	Elastic fundamental period T_s (s)	Model
0.05	40	45	$V_s = 400$ m/s, $c = 5$ kPa, $\phi = 44^\circ$	5	0.050	m5
	40	45	$V_s = 400$ m/s, $c = 50$ kPa, $\phi = 25^\circ$	16	0.160	m6
0.1	20	45	$V_s = 400$ m/s, $c = 5$ kPa, $\phi = 44^\circ$	4	0.040	m3
	20	45	$V_s = 400$ m/s, $c = 30$ kPa, $\phi = 25^\circ$	10	0.100	m4
0.15	20	30	$V_s = 250$ m/s, $c = 0.5$ kPa, $\phi = 37^\circ$	2	0.032	m1
	20	30	$V_s = 250$ m/s, $c = 15$ kPa, $\phi = 25^\circ$	8	0.130	m2
0.2	40	30	$V_s = 400$ m/s, $c = 30$ kPa, $\phi = 25^\circ$	15	0.150	m11
	20	15	$V_s = 150$ m/s, $c = 15$ kPa, $\phi = 18^\circ$	14	0.373	m12
0.25	40	15	$V_s = 150$ m/s, $c = 30$ kPa, $\phi = 18^\circ$	26	0.690	m7
	40	15	$V_s = 150$ m/s, $c = 0.5$ kPa, $\phi = 27^\circ$	5	0.130	m8
0.3	40	30	$V_s = 400$ m/s, $c = 5$ kPa, $\phi = 44^\circ$	4	0.040	m9
	20	15	$V_s = 250$ m/s, $c = 15$ kPa, $\phi = 24^\circ$	14	0.224	m10

in Europe, www.share-eu.org) (Table 4). The input accelerograms represent motions from moment magnitudes, M_w , varying from 5 to 7.62 recorded at epicentral distances, R , between 3.4 and 71.4 km with shear wave velocity at the first 30 m, $V_{s,30}$, between 602 and 2016 m/s. The input peak ground acceleration (PGA) values range from 0.065 to 0.91 g, the peak ground velocity (PGV) values range from 3.1 to 78.5 cm/s, the mean period T_m ranges from 0.16 to 1.14 s and the arias intensity I_a ranges from 0.015 to 10.97 m/s. Figure 2 presents relative scatter plots of M_w – $\ln R$, $\ln(\text{PGA})$ – $\ln(\text{PGV})$, $\ln(\text{PGA})$ – $\ln(T_m)$ and $\ln(\text{PGA})$ – $\ln(I_a)$ describing the distributions of the main ground motion parameters. To obtain the appropriate input motion at the base of the FLAC2D model, the selected time histories are first subjected to baseline correction and filtering ($f_1 = 0.25$ Hz, $f_2 = 10$ Hz) to assure accurate representation of wave transmission through the model. Moreover, due to the compliant base used in the model, the appropriate input excitation corresponds to the upward propagating wave train that is taken as one-half the target outcrop motion (Mejia and Dawson 2006).

Prior to the dynamic simulations, a static analysis is carried out to establish the initial effective stress field throughout the model. It is noticed that only the cases that result to nonzero displacement (≥ 0.001 m) due to seismic loading are addressed. Thus, the number of dynamic analyses performed for each model depends on the considered k_y value in relation to the PGA values of the selected input motions (see Table 4; Fig. 2). For instance, 40 dynamic analyses were carried out for model m6 ($k_y = 0.05$, see Table 2) while 13 analyses were possible for model m10 ($k_y = 0.3$, see Table 2).

4 Comparison of the numerical approach with empirical Newmark-type methods

The dynamic analysis results are extracted in terms of permanent horizontal displacements within the sliding mass for the idealized step-like slopes, characterized by different flexibility and resistance of the potential sliding surface. Thus, the variation of permanent horizontal displacements across the slope depends on the considered slope soil model. The sandy slope soil materials (e.g. models m1, m3, m5, m8, m9) are generally associated with thinner and shallower sliding surfaces and consequently to more condensed displacement field. On the contrary, larger and deeper sliding surfaces corresponding to more extended displacement field are shown for the clayey slope soil materials (e.g. models m2, m4, m6, m7, m10, m11, m12). “Average” values of the horizontal displacements are considered for the comparison with the empirical methods as well as for the derivation of the analytical expressions to account for the variation of the displacements within the sliding mass. In particular, the maximum computed horizontal displacements within the sliding mass were appropriately reduced, multiplied by a reduction factor equal to 0.65, to account for the fact that the sliding mass is deformable and that the maximum horizontal displacements act only in a rather small part of the sliding mass. Considering that the numerically computed horizontal displacements will be used to propose closed form analytical expressions for the average co-seismic slope displacements, it would be conservative to use the maximum computed horizontal displacement values. It’s worth noting that the use of the aforementioned reduction factor in the maximum computed horizontal displacements has been shown to yield a realistic approximation of the average response of the sliding mass in terms of permanent horizontal displacements in all analysis models.

Table 3 Soil properties

	Elastic bedrock		Intermediate layer		Surface layer				
			Stiff clay	Dense sand	Stiff clay	Relatively dense sand	Relatively stiff clay	Loose sand	Soft clay
Dry density (kg/m ³)	2300		2000	2000	2000	1800	1800	1700	1700
Young's modulus (KPa)	4.32E+06		1.30E+06	8.32E+05	8.32E+05	2.93E+05	2.93E+05	9.95E+04	9.95E+04
Poisson's ratio	0.3		0.3	0.3	0.3	0.3	0.3	0.3	0.3
Shear modulus (KPa)	1.66E+06		5.00E+05	3.20E+05	3.20E+05	1.13E+05	1.13E+05	3.83E+04	3.83E+04
Cohesion (KPa)	–		50	5	30–50	0.5	15	0.5	15–30
Friction angle (°)	–		27	44	25	37	24–25	27	18
Dilation angle (°)	–		0	0	0	0	0	0	0
Shear wave velocity Vs (m/s)	850		500	400	400	250	250	150	150

Table 4 Seismic records used for the numerical analyses

Date	Earthquake name	Station country	M_w	R (km)	Preferred FS	Station name	$V_{s,30}$ (m/s)	Database code
25/7/2003	N Miyagi Prefecture	Japan	6.1	32.00	Reverse	Oshika	1432.7	C&F_277
23/10/2004	Mid Niigata Prefecture	Japan	6.6	36	Reverse	Tsunan	626	C&F_324
12/6/2005	Anza	USA	5.2	11.50	Strike-slip	Phynon Flat Observatory	724.9	C&F_1008
22/12/2003	San Simeon	USA	6.4	61.5	Reverse	Ca: San Luis Obispo; Rec Center	712.8	C&F_1017
16/9/1978	Tabas	Iran	7.35	57	Oblique	Tabas	712	ESMD_60
10/6/1987	Kalamata (Aftershock)	Greece	5.36	17.00	Oblique	Kyparrisia-Agriculture Bank	778.0	ESMD_126
13/5/1995	Kozani	Greece	6.61	17	Normal	Kozani	1000	ESMD_171
15/4/1979	Montenegro	Serbia and Montenegro	6.9	65	Thrust	Herecnovi Novi-O.S.D. Pavivic School	875	ISESD_225
7/9/1999	Ano Liosia	Greece	6.04	17.00	Normal	Athens 4 (Kipseli District)	934.0	ESMD_335
25/10/1984	Kremidia (Aftershock)	Greece	5	16		Pelekanada-Town Hall	1530	ISESD_576
13/10/1997	Kalamata	Greece	6.4	48	Thrust	Koroni-Town Hall (Library)	1530	ISESD_1579
17/5/1995	Kozani (Aftershock)	Greece	5.3	16.00	Normal	Chromio-Community Building	623.0	ISESD_1210
6/5/1976	Friuli	Italy	6.4	21.70	Reverse	Tolmezzo-Diga Ambiesta	1029.6	ITACA_16
15/9/1976	Friuli (Aftershock)	Italy	5.9	8.50	Reverse	Tarcento	901.0	ITACA_116
23/11/1980	Irpinia	Italy	6.9	28.30	Normal	Bisaccia	976.2	ITACA_180
14/10/1997	Umbria Marche (Aftershock)	Italy	5.6	20.00	Normal	Norcia	681.2	ITACA_491
9/9/1998	App. Lucano	Italy	5.6	6.60	Normal	Lauria Galdo	603.2	ITACA_613
6/4/2009	L. Aquila Mainshock	Italy	6.3	4.40	Normal	L. Aquila—V. Aterno—Colle Grilli	684.8	ITACA_857
9/2/1971	San Fernando	USA	6.61	20.04	Reverse	Lake Hughes #12	602.1	NGA_71
28/11/1974	Hollister-03	USA	5.14	11.08	Strike-slip	Gilroy array #1	1428.1	NGA_98
6/8/1979	Coyote Lake	USA	5.74	4.37	Strike-slip	Gilroy array #6	663.3	NGA_150
2/5/1983	Coalinga-01		6.36	33.52	Reverse	Slack Canyon	684.93	NGA_369

Table 4 continued

Date	Earthquake name	Station country	M_w	R (km)	Preferred FS	Station name	$V_{s,30}$ (m/s)	Database code
24/4/1984	Morgan Hill	USA	6.19	36.34	Strike-slip	Gilroy array #6	663.3	NGA_459
23/12/1985	Nahanni, Canada		6.76	6.8	Reverse	Site 1	659.6	NGA_495
14/11/1986	Taiwan Smart1 (45)		7.3	71.35	Reverse	Smart1 E02	659.6	NGA_572
7/2/1987	Baja California		5.5	3.69	Strike-slip	Cerro Prieto	659.6	NGA_585
18/10/1989	Loma Prieta	USA	6.93	35.47	Reverse-oblique	Gilroy array #6	663.3	NGA_769
18/10/1989	Loma Prieta	USA	6.93	16.34	Reverse-oblique	Usc Lick observatory	659.6	NGA_810
25/4/1992	Cape Mendocino		7.01	4.51	Reverse	Petrolia	712.82	NGA_828
28/6/1992	Landers		7.28	44.02	Strike-slip	Lucerne	684.94	NGA_879
17/1/1994	Northridge-01	USA	6.69	25.42	Reverse	La-Griffith Park observatory	971.4	NGA_994
17/1/1994	Northridge-01	USA	6.69	20.36	Reverse	Pacoima Dam (Downstr)	2016.1	NGA_1050
16/1/1995	Kobe, Japan		6.9	8.7	Strike-slip	Nishi-Akashi	609	NGA_1111
20/9/1999	Chi-Chi, Taiwan		7.62	15.42	Reverse-oblique	Tcu071	624.85	NGA_1507
28/6/1991	Sierra Madre		5.61	6.46	Reverse	Mt Wilson—Cit Seis Sta	821.69	NGA_1645
16/10/1999	Hector Mine		7.13	26.53	Strike-slip	Hector	684.93	NGA_1787
20/9/1999	Chi-Chi, Taiwan-03		6.2	18.5	Reverse	Tcu129	664.43	NGA_2658
17/8/1999	Izmit	Turkey	7.6	42.77	Strike-slip	Gebeze-Tubitaak Marmara Arastirma Merkezi	700.9	T-NSMP_1105
17/8/1999	Izmit	Turkey	7.6	3.40	Strike-slip	Izmit-Meteoroloji Istasyonu	827.3	T-NSMP_1109
12/11/1999	Duzce 1	Turkey	7.1	15.60	Strike-slip	Ldeo Station No. C1058 Bv	718.9	T-NSMP_1583

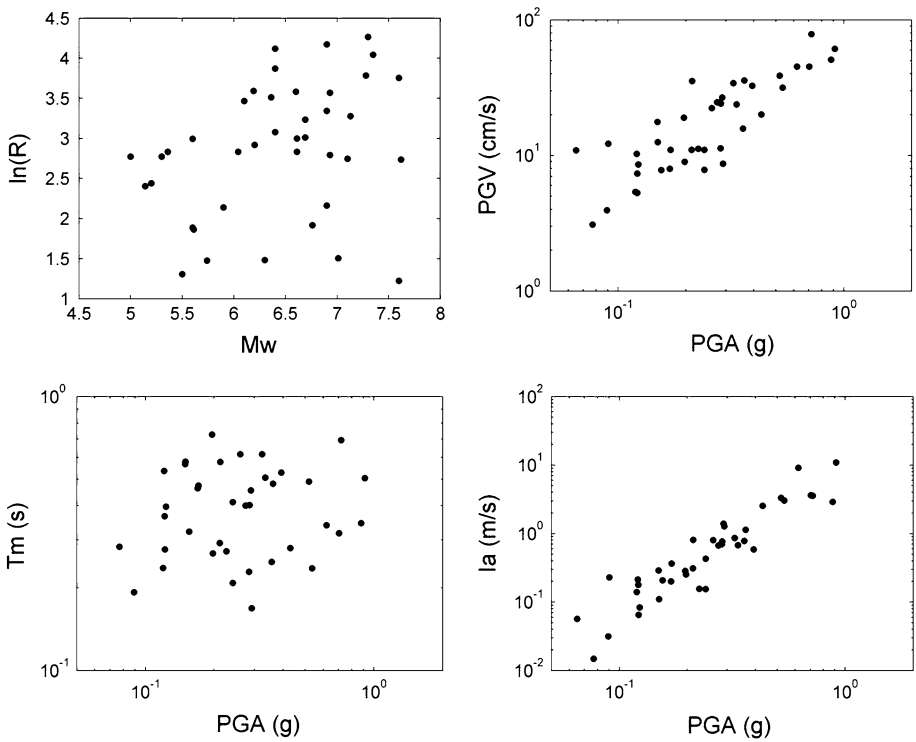


Fig. 2 Distributions of the main ground motion parameters

Figure 3 presents the distribution of the “average” values of the numerical horizontal displacements in log space that vary from very small values (smaller than 0.01 m) to large ones (>1 m). In total, 285 nonzero permanent horizontal displacements are calculated for all considered analysis cases.

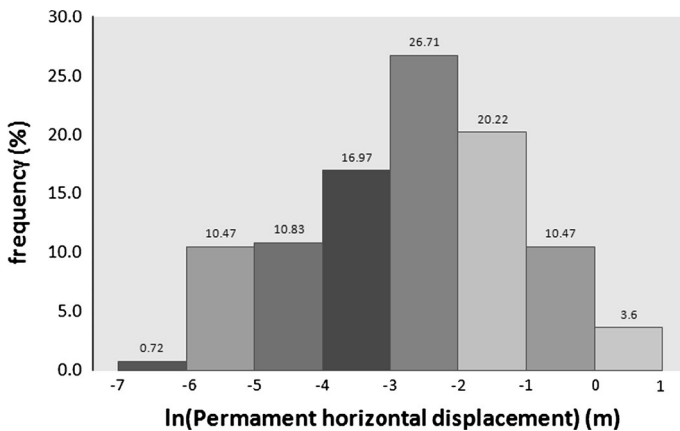


Fig. 3 Histogram of the computed numerical horizontal displacements (for all models, $N = 285$)

These displacements are then compared with the slope displacement (D) predicted with four empirical models commonly used in earthquake engineering practice, i.e. the conventional analytical Newmark rigid block model (Newmark 1965), Jibson (2007) rigid block model, Rathje and Antonakos (2011) decoupled sliding block model and Bray and Travararou (2007) coupled stick–slip sliding block model. The main modeling assumptions and input parameters of these methods have been discussed in Sect. 2. This comparison aspires not only to enhance the reliability of the numerical analysis results but also to assess the relative accuracy of the different displacement based approaches with respect to the present a priori more advanced numerical approach. It is noted that Newmark-type methods capture the part of seismically induced displacement attributed to the deviatoric induced deformation while the corresponding part attributed to the volumetric compression is not account for. This displacement due to deviatoric deformation is largely horizontal (Bray and Travararou 2007) justifying the use of the horizontal (instead of the vector) numerical displacement for the comparison.

To derive the appropriate inputs for the Newmark-type methods that include the effect of soil conditions, and to allow a direct comparison with the numerical results, the acceleration time histories and the corresponding intensity parameters at the depth of the sliding surface were computed through a one-dimensional (1D) non-linear site response analysis using FLAC 2D considering the same soil properties as in the 2D dynamic analysis (Fig. 4). In particular, as for 2D analysis, 12 1D soil models are constructed that are then subjected to the same recorded earthquake motions described previously. It is noticed that the 1D soil profile is located at the section that approximately corresponds to the maximum slide mass thickness H of the potential sliding surface (section A in Fig. 4). The maximum slide mass thickness H (or otherwise the maximum depth of the sliding surface, see Table 2), which is calculated by means of pseudostatic slope stability analysis for the critical sliding surface, varies between 2 and 26 m for the different analyzed slope cases.

Figure 5 presents correlations between the ground motion intensity parameters of the input motion at the rock outcrop and the corresponding intensity parameters at the depth of the sliding surface calculated via 1D dynamic analysis. It is seen that all intensity parameters display a considerable variability with respect to the considered site conditions (soil or rock). A linear regression fit of the logarithms of the IM, rock–IM, soil which minimizes the regression residuals is suggested for all IMs as shown in the figure. Such log-linear relationships could be used in practice to calculate the required IMs for soil

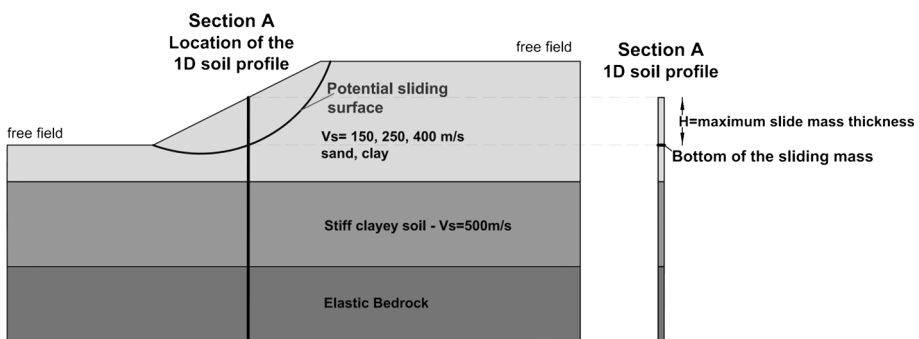


Fig. 4 Schematic view of the model used to perform the 1D dynamic analyses

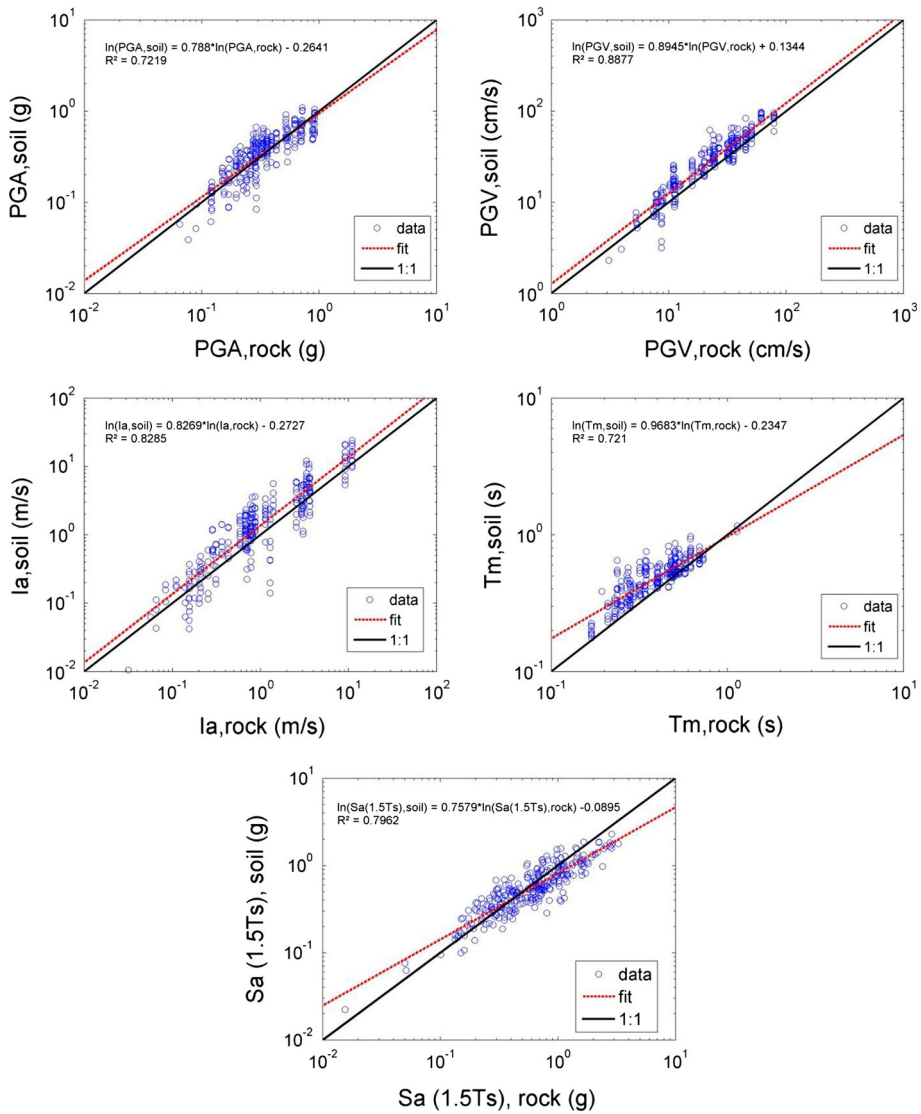


Fig. 5 Variation of peak ground acceleration, peak ground velocity, Arias intensity, mean period and spectral acceleration at $1.5T_s$ of the input outcropping accelerograms (PGA,rock; PGV,rock; Ia,rock; Tm,rock, Sa(1.5Ts),rock) with the corresponding calculated peak ground acceleration, peak ground velocity, Arias intensity, mean period and spectral acceleration at $1.5T_s$ at the depth of the sliding surface (PGA,soil; PGV,soil; Ia,soil; Tm,soil, Sa(1.5Ts),soil)

conditions (e.g. at the bottom of the potential sliding mass) given the corresponding IMs at the rock outcrop. The latter parameters are normally more easily obtained from a seismic hazard analysis. It is noted, however, that these equations are valid within the range of the input ground motion parameters considered in this study and should not be used outside of this range.

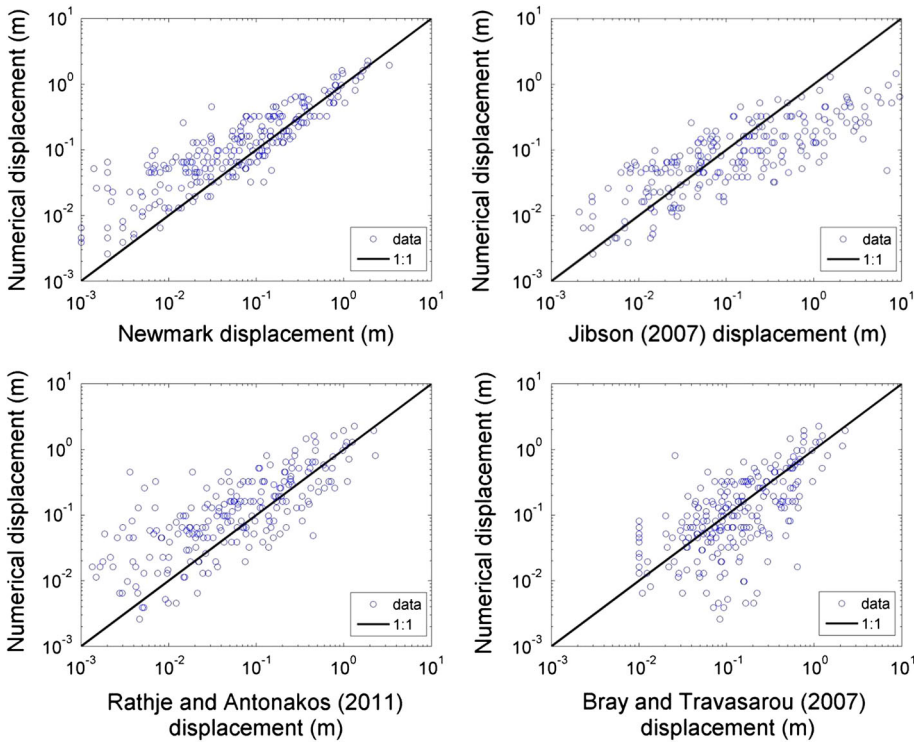


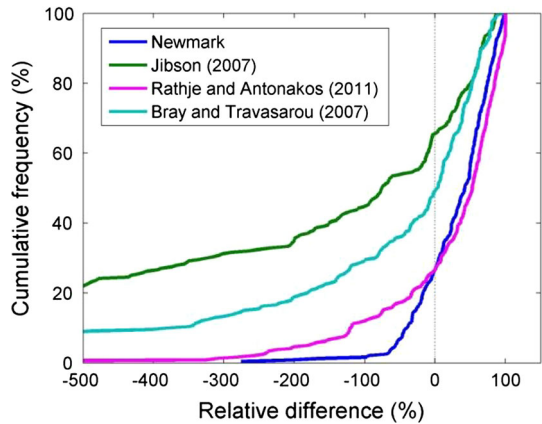
Fig. 6 Numerically versus empirically calculated displacements

Figure 6 shows a direct comparison between analytical Newmark’s, Jibson (2007) Bray and Travararou (2007) and Rathje and Antonakos (2011) displacements with the horizontal displacements calculated from the 2D dynamic numerical analyses. It is observed that numerical displacements generally are not inconsistent with the predicted Newmark-type displacements enhancing the reliability and robustness of the dynamic analysis results. In particular, the following general observations can be deduced from Fig. 6: (1) Newmark method generally predicts smaller displacements compared to the numerical model, (2) Jibson (2007) model tends to underpredict small numerical displacements and overpredict large displacements, (3) Rathje and Antonakos (2011) model goes relatively well with respect to the numerical analysis except for a group of under-predicted displacements at the small displacement range, and finally (4) Bray and Travararou (2007) model is generally in good agreement with the numerical analysis although its ability to predict very small displacements cannot be assessed as it cannot predict displacements smaller than 0.01 m.

It is noted that cases where Bray and Travararou (2007) model computed “zero displacement” (i.e. <0.01 m) and FLAC analysis did not, were not considered for the comparisons as they cannot be plotted in Fig. 6. To have a common dataset for all methods, these cases have also been excluded from the comparison with the other empirical methods.

A relatively large dispersion in the displacement estimation is shown. This dispersion is also displayed in Fig. 7, which presents the cumulative distribution of the *relative difference* (Relative difference (%) = $\frac{D_{\text{numerical}} - D_{\text{empirical}}}{D_{\text{numerical}}} \cdot 100\%$) between the numerical and

Fig. 7 Cumulative distribution of the *Relative difference (%)* between numerical and empirical slope displacements for each of the empirical sliding block models



empirical slope displacements for each of the empirical sliding block model. Similar cumulative distribution functions were presented in Meehan and Vahedifard (2013) to compare the predictions of various simplified empirical displacement based models with the actual observed displacement. It is noted that for positive values of the *relative difference* the empirical methods underpredict the displacements derived from the numerical analysis and vice versa.

By examining the cumulative distribution functions it is seen that Newmark analytical rigid block model and Rathje and Antonakos (2011) decoupled model generally tend to predict smaller displacements compared to the numerically derived ones. In particular, positive values of the *relative difference* in the displacement prediction are presented for cumulative frequencies from around 20–30 to 100 %. On the other hand, Bray and Travararou (2007) coupled model may either overpredict or underpredict the numerical displacements yielding positive values of the *relative difference* in the displacement prediction for cumulative frequencies from around 49 to 100 %. This is in line with the inherent coupled stick–slip assumption adopted in the method that offers a conceptual improvement over the rigid block and decoupled approaches for modeling the physical mechanism of earthquake-induced slope displacement. Finally, Jibson (2007) simplified rigid block model tends to predict larger displacements compared the numerically calculated ones dominated by negative predictions of the *relative difference* for cumulative frequencies up to 65 %. The latter model is also associated with a very large dispersion in the median displacement estimation with respect to the numerical analysis compared to the former ones. This dispersion is obvious in the cumulative distribution of the *relative difference* diagram resulting to *relative differences* greater than -500% for cumulative frequencies up to 20 %. This observation confirms Jibson’s statement concerning the avoidance of using his regression equations for site-specific applications (e.g. for design purposes) where accurate estimates of displacement are required. Instead, he states that they could be used in regional-scale assessment and mapping of seismic landslide hazards.

After analyzing all data a distinction is also made between stiff ($T_s < 0.2$ s) and flexible ($T_s > 0.2$ s) slopes as well as between weak ($k_y \leq 0.1$) and high strength ($k_y > 0.1$) slopes. Figures 8 and 9 show correlations between numerically and empirically estimated displacements for varying T_s and k_y values respectively.

It is seen that all empirical models generally tend to underpredict the numerical displacements for flexible slopes presenting positive values of *relative difference* in the

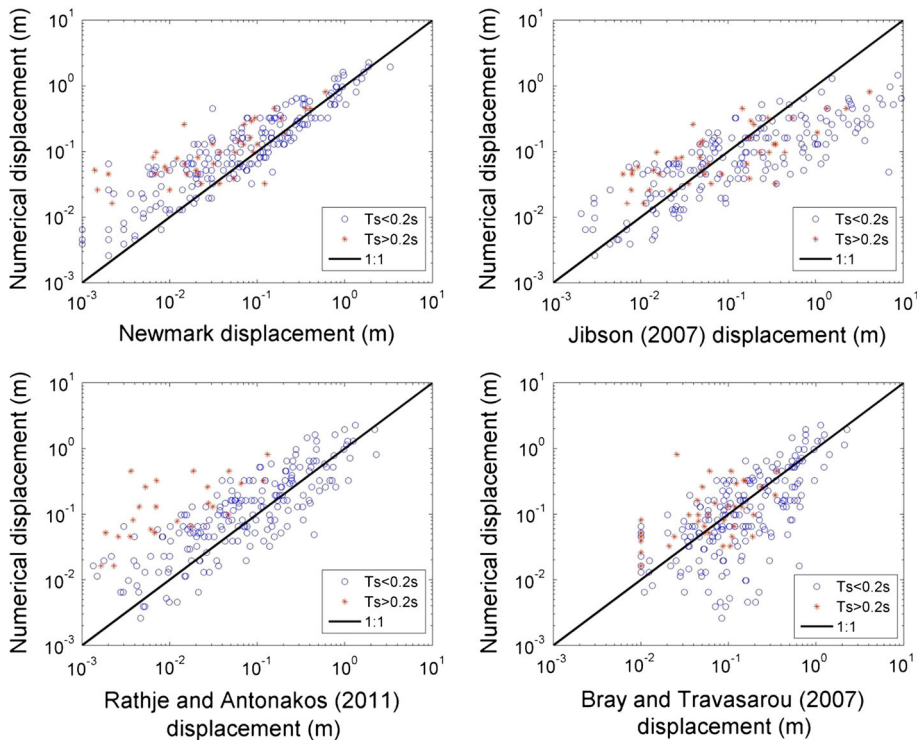


Fig. 8 Numerically versus empirically calculated displacements for stiff and flexible sliding masses

displacement prediction for cumulative frequencies from around 0–45 to 100 % (see Fig. 10, right).

For stiff sliding masses, Newmark and Rathje and Antonakos (2011) models generally tend to underestimate the numerically derived displacements whereas Jibson (2007) severely overpredicts the corresponding displacements. Bray and Travarasrou (2007) method predicts median displacements (cumulative frequency 50 %) that are in good agreement with the ones calculated by the numerical analysis (see Fig. 10, left).

For weak slopes, Newmark and Rathje and Antonakos (2011) models show good correlations with respect to the dynamic analysis, while Jibson (2007) and Bray and Travarasrou (2007) models predict greater displacements (see Fig. 11, left).

Finally, for high strength slopes, Newmark, Rathje and Antonakos (2011) and Bray and Travarasrou (2007) models tend to underestimate the numerically calculated displacements while Jibson (2007) model presents median displacement predictions that are in accordance with the numerical ones (see Fig. 11, right).

In all considered cases, among the four models, Newmark’s analytical approach presents the minimum dispersion. This trend may prove the superiority of the analytical over the simplified approaches as the latter are “models of models” that are subjected to additional assumptions associated with reducing the analytical approach into a simplified mathematical equation.

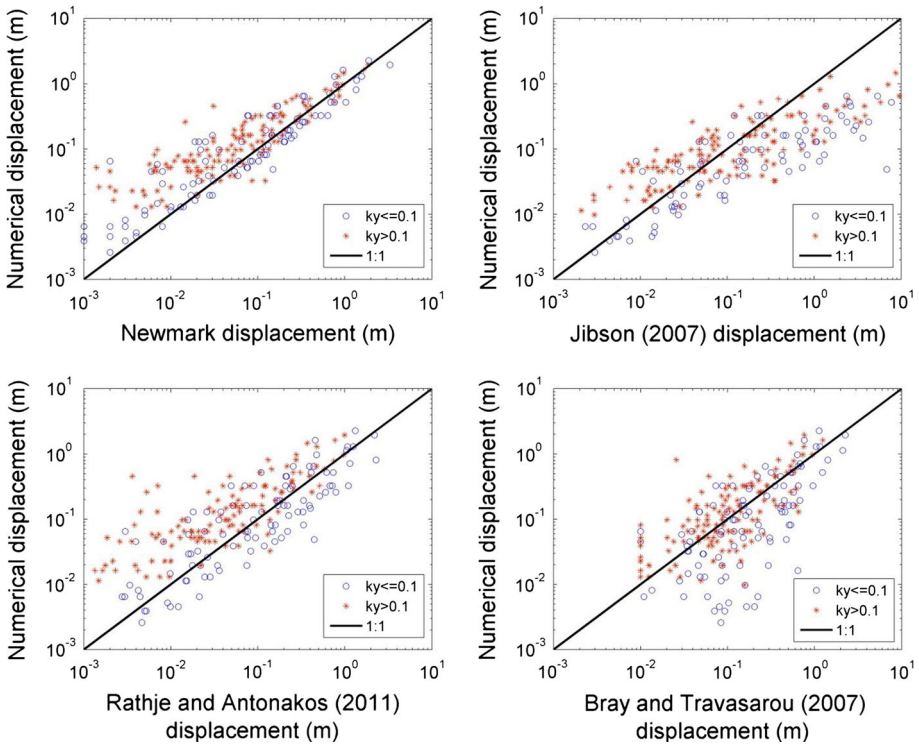


Fig. 9 Numerically versus empirically calculated displacements for weak and high strength sliding masses

5 Predictive models for assessing seismic displacement using numerical analysis data

5.1 Development of regression models using optimal scalar intensity measures

Uncertainty in the ground motion characterization is the greatest source of uncertainty in calculating earthquake induced slope displacements (Bray 2007). Thus, the selection of appropriate IMs is important to increase the accuracy of the predictive analytical relationships of seismic permanent displacement. The selection of the proposed IMs is also important to reduce the overall computation effort, as fewer ground motions are required to achieve the desired accuracy.

The optimal IM is identified through regression analyses correlating the numerically calculated seismically induced slope displacements (D) and various IMs, namely PGA, PGV, I_a , T_m , $S_a(1.5T_s)$. These are some of the most frequently used IMs in earthquake engineering practice representing different aspects of the ground motion characteristics (i.e. intensity, frequency content and duration). In particular, PGA characterizes the earthquake ground motion peak amplitude (amplitude/intensity), PGV the intensity and frequency content of the earthquake motion, I_a the intensity and implicitly the duration of the ground motion, T_m the earthquake frequency content and finally $S_a(1.5T_s)$ is related to both the ground motion intensity and the frequency characteristics of the sliding mass. It is

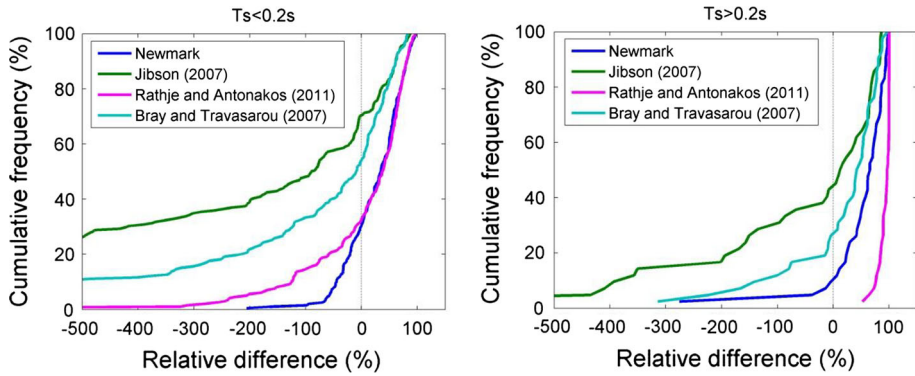


Fig. 10 Cumulative distribution of the *Relative difference* (%) between numerical and empirical slope displacements for each of the empirical sliding block models for stiff ($T_s < 0.2$ s) and flexible ($T_s > 0.2$ s) sliding masses

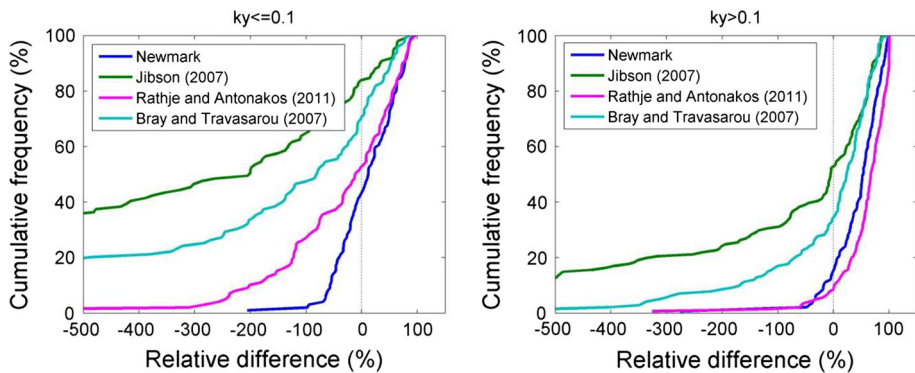


Fig. 11 Cumulative distribution of the *Relative difference* (%) between numerical and empirical slope displacements for each of the empirical sliding block models for weak ($k_y \leq 0.1$) and high strength ($k_y > 0.1$) sliding masses

noted that the ratio k_y/PGA is also used as an IM as it provides a direct assessment of whether the displacement will be greater than zero (i.e. for $\text{PGA} > k_y$, $D > 0$ and 0 otherwise) (Saygili and Rathje 2008). It is also worth mentioning that the estimated IMs at the depth of the sliding surface estimated via the 1D dynamic analyses (Sect. 4), which account for the affect of soil conditions (including soil classes B, C and D according to EC8), are used in the regressions. Considering the fact that seismic motions are essentially recorded at the ground surface, IMs at the free-field ground surface are suggested in practice without any depth modification. This is in line with previous studies (e.g. Bray and Travararou 2007; Rathje and Antonakos 2011) and as discussed in Bray and Travararou (2007) is considered a relatively “conservative” hypothesis. In cases, however, where the IMs for soil conditions cannot be accurately estimated or for more generic applications, simplified relationships that yield the IMs for soil conditions (e.g. at the depth of the sliding surface) given the corresponding IMs at the rock outcrop are proposed (see Sect. 4).

In this study IMs were rated based on two different criteria: proficiency (i.e. a composite measure of efficiency and practicality) (Padgett et al. 2008) and sufficiency (Luco and Cornell 2007). Proficiency serves as the primary factor in the selection process for an

optimal IM while sufficiency is a secondary factor, which further supports the selection of appropriate IMs.

A power model is first used to describe the relationship between the seismic slope displacement D and the various IMs:

$$D = a \cdot \text{IM}^b \quad (1)$$

where a and b are coefficients defined by the regression.

This can be rearranged to perform a linear regression of the logarithms of the IMs and the response quantity (seismic slope displacement) to establish a demand model of the following form:

$$\ln(D) = b \cdot \ln(\text{IM}) + \ln(a) + \varepsilon \cdot \sigma \quad (2)$$

where D is the seismically induced slope displacement (in m), ε is the standard normal variant with zero mean and unit standard deviation. The dispersion term sigma (σ) represents the conditional standard deviation of the regression (in natural log units) and is a metric of the efficiency of the IM with respect to the demand parameter (seismic slope displacement). Lower σ values yields less dispersion about the estimated median in the results indicating a more efficient IM.

The regression parameter b in Eq. 2 is a metric of the practicality of the IM. Practicality describes the dependence of the level of the slope displacement upon the level of the IM. When this parameter approaches zero the IM term contributes negligibly to the demand estimate and thus a lower b value implies a less practical IM (Padgett et al. 2008).

For an optimal IM selection, the term proficiency is introduced (Padgett et al. 2008) which measures the composite effect of efficiency and practicality. A more proficient IM is characterized by a lower modified dispersion ζ and is estimated as follows:

$$\zeta = \sigma/b \quad (3)$$

Figure 12 presents correlations between the slope displacements and the various considered IMs along with the curves fit using Eq. 2.

Table 5 lists the parameters of the demand models from Eq. 2 as well as their proficiency. As shown in the table, PGV and I_a are the most efficient IMs whereas PGV is the most proficient one followed by PGA and k_y/PGA (shown in bold in Table 5). Thus, although I_a is an efficient IM, it is not practical (low b value) and therefore it should not be considered an optimal IM.

A sufficient IM is conditionally statistically independent of ground motion characteristics, such as magnitude (M) and epicentral distance (R) (Luco and Cornell 2007). In this study, the sufficiency is evaluated by performing a regression analysis on the residuals, ε/IM , from the calculated seismic slope displacements relative to the ground motion characteristic, M or R (see Figs. 13, 14). A small p value for the linear regression of the residuals on M or R is indicative of an insufficient IM, in which the coefficient of the regression estimate is statistically significant. The cutoff for an insufficient IM is assumed to be a p value of 0.10. For PGA, PGV, $S_a(1.5T_s)$ and k_y/PGA , the mean residuals do not vary with distance (p value >0.10), but they increase with increasing magnitude (p value ~ 0). On the other hand, I_a is statistically independent from magnitude (p value = 0.70) but it depends on epicentral distance (p value <0.10) while T_m is dependent both on magnitude and epicentral distance (p value ~ 0). These trends indicate that none of the selected IMs satisfies the sufficiency criterion with respect to magnitude and epicentral distance in a rigorous way.

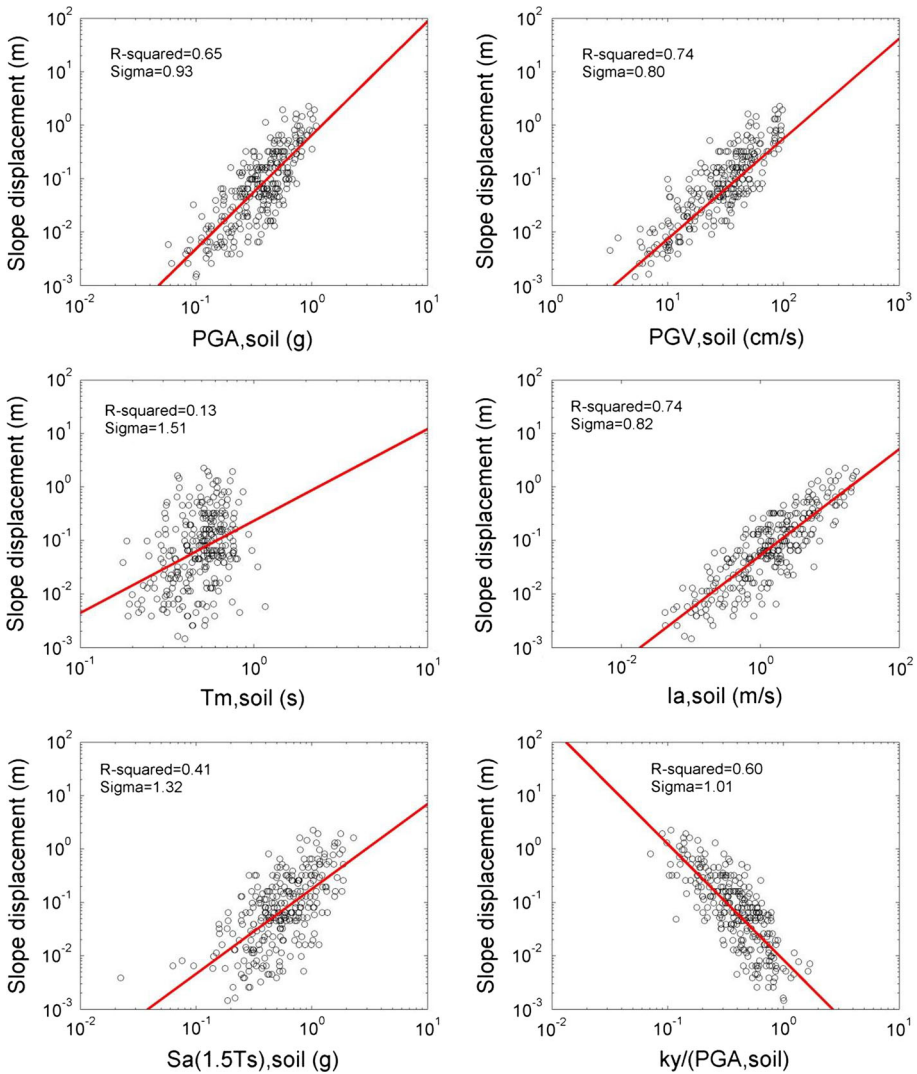


Fig. 12 Regression of seismic slope displacement for quantifying the efficiency and practicality of different IMs

Table 5 Demand models and their efficiency, practicality and proficiency for the different considered IMs

IM	$\ln(a)$	b	σ	ζ
PGA (g)	-0.428	2.127	0.93	0.44
PGV (cm/s)	-8.892	1.873	0.80	0.43
T_m (s)	-1.455	1.717	1.46	0.85
I_a (m/s)	-2.944	0.993	0.82	0.82
$S_a(1.5T_s)$	-1.716	1.588	1.21	0.76
k_y/PGA	-4.770	-2.165	1.01	0.46

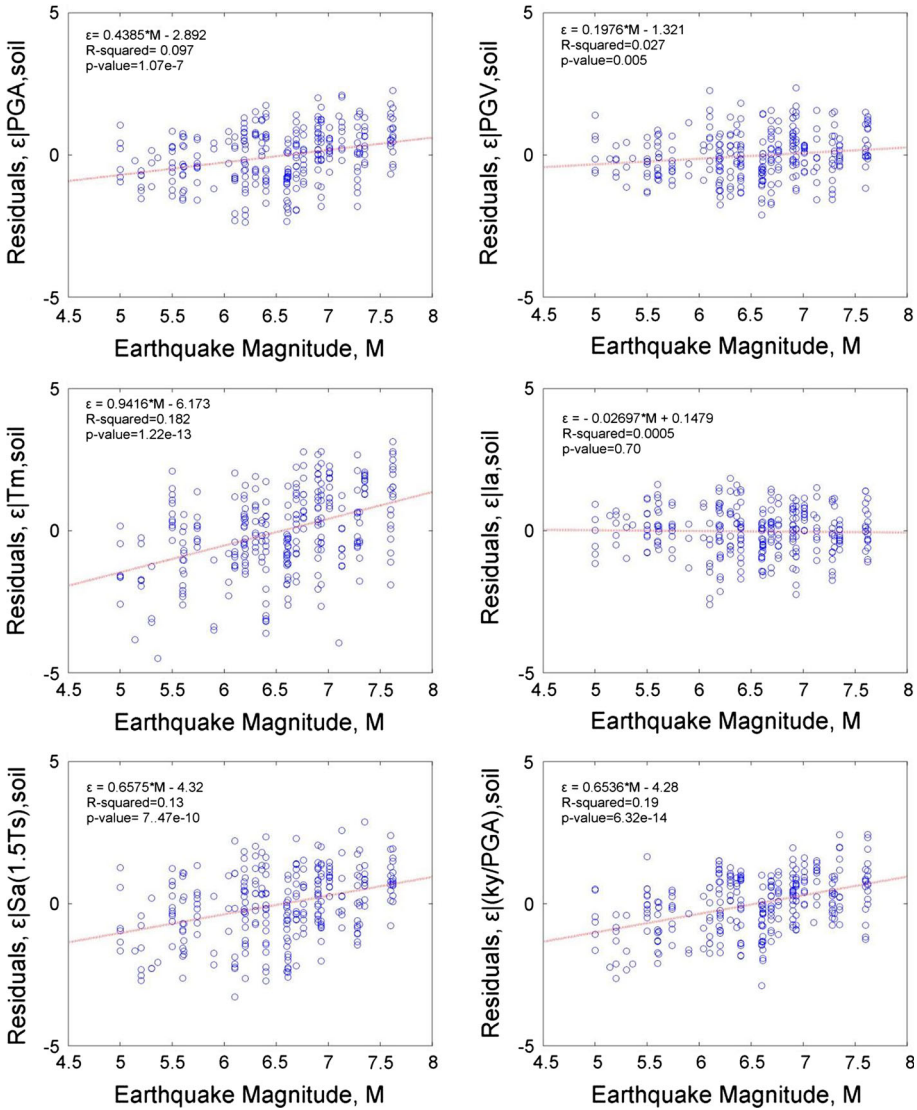


Fig. 13 Sufficiency of the studied IMs by examining the conditional statistical independence from magnitude

However, as shown by Shome (1999), the error in the prediction of the demand parameter (seismic slope displacement in our case) using a hazard decoupling assumption with an insufficient IM can be as small as $\pm 10\%$. Considering that scalar IMs are proposed to assess slope displacement based only on the proficiency criterion. In particular, the most proficient IMs, i.e. PGV, PGA and k_y/PGA , are suggested to correlate to slope displacements using the functional form described in Eq. 2.

The yield coefficient k_y , which represents the overall dynamic resistance of the slope, has been always used in sliding block procedures due to its important effect on seismically

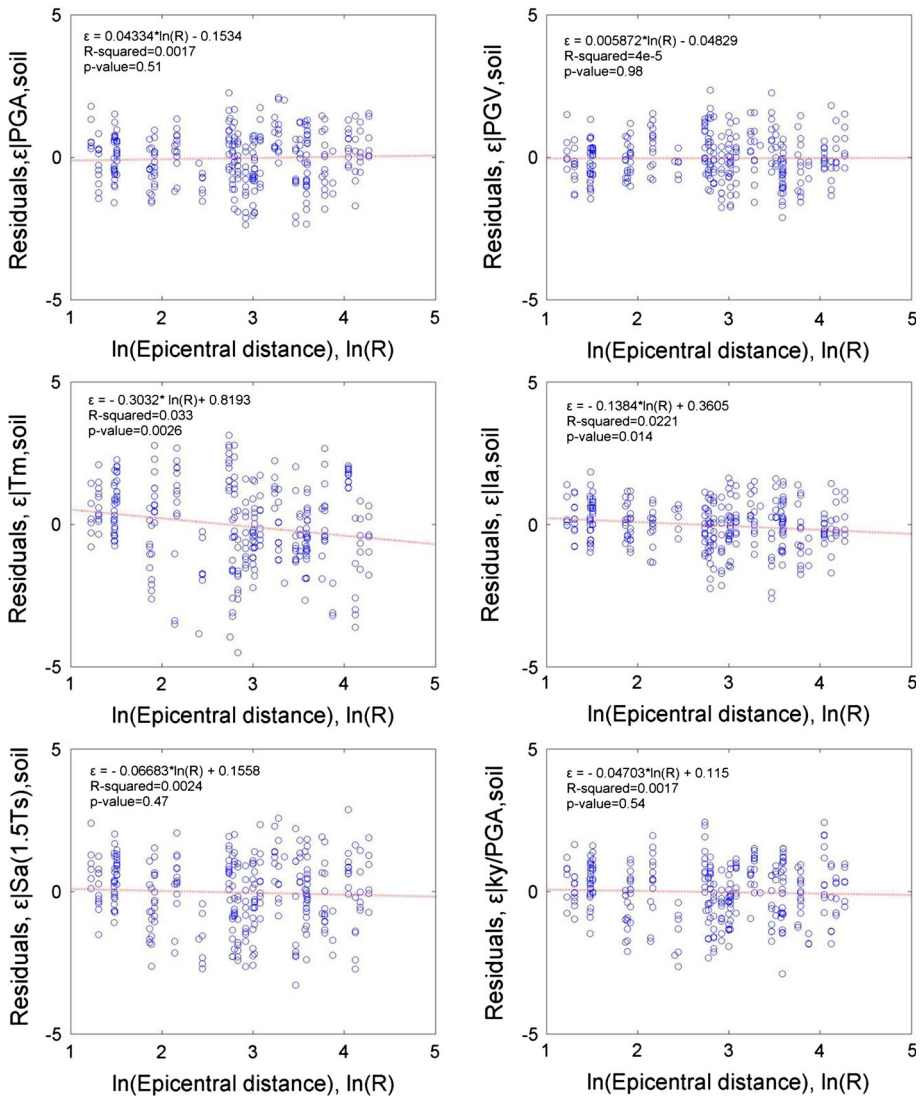


Fig. 14 Sufficiency of the studied IMs by examining the conditional statistical independence from epicentral distance

induced slope displacement (Bray 2007). In this respect, k_y is also added to the regression equation:

$$\ln(D) = b \cdot \ln(IM) + \ln(a) + c \cdot k_y + \epsilon \cdot \sigma \tag{4}$$

A linear dependence of the residuals for the considered IMs on k_y is taken into account as shown in Eq. 4.

The proposed regression parameters for the most proficient IMs, i.e. PGV, PGA and k_y /PGA are presented in Table 6. It is seen that the models display significantly less variability when considering k_y term in the regression.

Table 6 Demand models for most proficient IMs when considering the k_y term in the regression equation

IM	$\ln(a)$	b	c	σ
PGA (g)	0.529	2.127	-6.583	0.80
PGV (cm/s)	-8.028	1.873	-5.964	0.68
k_y /PGA	-5.965	-2.165	7.844	0.82

Table 7 Demand models for most proficient IMs when considering both the k_y and the magnitude term in the regression equation

IM	$\ln(a)$	b	c	d	σ
PGA (g)	-2.965	2.127	-6.583	0.535	0.72
PGV (cm/s)	-9.891	1.873	-5.964	0.285	0.65
k_y /PGA	-10.246	-2.165	7.844	0.654	0.75

Finally, taking into account the dependence of the residuals for almost all considered IMs (i.e. PGV, PGA, k_y /PGA, T_m and $S_a(1.5T_s)$) on magnitude, magnitude term is also added to the regression equation to eliminate bias due to magnitude:

$$\ln(D) = b \cdot \ln(IM) + \ln(a) + c \cdot k_y + d \cdot M + \varepsilon \cdot \sigma \quad (5)$$

A linear dependence of the residuals for the IMs on magnitude is considered as shown in Eq. 5. It's worth noting that the inclusion of magnitude term in Eq. 4 captures in part the influence of the duration of the seismic motion in the seismically induced slope displacement estimation. The proposed regression parameters for the most proficient IMs, i.e. PGV, PGA and k_y /PGA, when considering also the magnitude dependence are presented in Table 7. As shown in the table, the efficiency of the demand models is further improved when considering the magnitude term. Based on the above considerations, these scalar models (Eq. 5; Table 7) are recommended for use in engineering applications. However, the demand models that do not include the magnitude term (Eq. 4; Table 6) could also be applied at projects where the inclusion of magnitude causes some complication.

5.2 Development of regression models using optimal vector intensity measures

The use of vector IMs enables the model to capture additional significant features of the ground motion (related to its amplitude, frequency content or duration), which affect the magnitude of the seismic slope displacement. Vector IMs were selected based on the proficiency (i.e. efficiency and practicality) of the scalar IMs, the correlation coefficient ρ_{IM_i, IM_j} between them as well as the overall efficiency of the vector model. Correlation coefficients were estimated using the methodology outlined by Baker and Cornell (2006). IMs with smaller correlation coefficients were selected as a smaller value of ρ_{IM_i, IM_j} indicates that the two IMs cover more complementary information about the ground motion parameters leading to a smaller standard deviation in the displacement prediction (Saygili and Rathje 2008). PGV is considered as the first component of the vector as it is the most proficient IM. Table 8 presents correlation coefficients between PGV and the remaining IMs. It is seen that the combination of PGV and k_y /PGA yields the lowest

Table 8 Correlation coefficients between PGV and the remaining IMs

IM ₁ /IM ₂	ρ_{IM_1,IM_2}				
	PGA	T _m	I _a	S _a (1.5T _s)	k _y /PGA
PGV	0.75	0.57	0.67	0.59	0.15

correlation coefficient. The functional form used for the regression on a vector of IMs is described as:

$$\ln(D) = \ln(a) + b \cdot \ln(IM_1) + e \cdot \ln(IM_2) + \varepsilon \cdot \sigma \tag{6}$$

where D is the seismically induced slope displacement (in m), IM₁ is the peak ground velocity, IM₂ is the second intensity measure and a, b, and e are regression coefficients.

Equation 6 was selected based on the observation that the residuals of the regression on PGV had only a linear dependence on the logarithm of the remaining IMs when plotted against them.

Table 9 presents the derived vector models along with their overall efficiency (defined by their σ values). As shown in the table, among the considered vector IMs, PGV–I_a and PGV–k_y/PGA are the most efficient ones (shown in bold in Table 9). It is seen that the efficiency of the vector IMs is improved compared to the corresponding scalar IMs (lower sigma values) (see Table 5).

However, it’s up to the engineer to decide on a project basis whether this improvement in efficiency by the use of a vector IM offsets the complexities in the vector seismic hazard evaluation associated with the computation of the joint annual probability of occurrence of the pairs of ground motion parameters (Travasarou and Bray 2003).

The sufficiency criterion is addressed by considering the magnitude and distance dependence of the residuals for each pair of IMs (see Figs. 15, 16). For all considered pairs of IMs, the mean residuals do not vary with distance (*p* value ≥ 0.10). However, only PGV–k_y/PGA and PGV–I_a pairs are statistically independent from magnitude (*p* value ≥ 0.10) and therefore only these IMs cover the sufficiency criterion. Thus the vectors IMs that may sufficiently predict seismic slope displacement are PGV–k_y/PGA and PGV–I_a. However, PGV–k_y/PGA pair has a correlation coefficient 0.15 that is indicative of intensity parameters that provide considerable complementary information about the ground motion as opposed to PGV–I_a pair that distinguishes a quite higher correlation coefficient (equal to 0.67) (see Table 8). In addition, PGV and k_y/PGA represent the most proficient scalar IMs; consequently the PGV–k_y/PGA pair is proposed as the most appropriate one to correlate to seismic slope displacements.

Table 9 Demand models and their associated efficiency for the different considered vector IMs

IM ₁	IM ₂	ln(a)	b	e	σ
PGV (cm/s)	k_y/PGA	−9.524	1.873	−0.634	0.70
PGV (cm/s)	T _m (s)	−9.250	1.873	−0.444	0.79
PGV (cm/s)	I_a (m/s)	−8.940	1.873	0.072	0.80
PGV (cm/s)	PGA (g)	−8.897	1.873	0.025	0.80
PGV (cm/s)	S _a (1.5T _s) (g)	−8.912	1.873	0.018	0.80

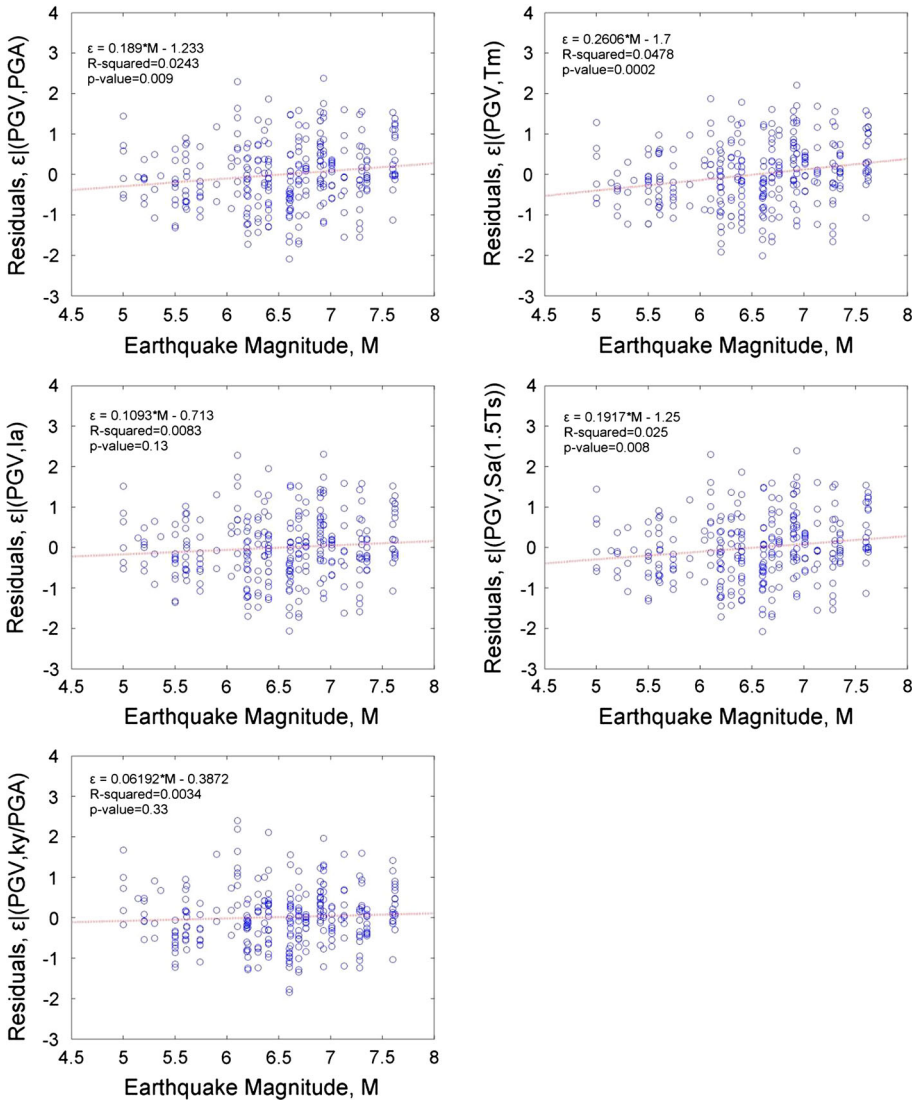


Fig. 15 Sufficiency of the studied vector IMs by examining the conditional statistical independence from magnitude

Finally, k_y term is also incorporated in Eq. 6 considering its importance in seismic slope displacement estimation. Thus the functional form for the regression on a vector of IMs becomes:

$$\ln(D) = \ln(a) + b \cdot \ln(IM_1) + e \cdot \ln(IM_2) + c \cdot k_y + \epsilon \cdot \sigma \tag{7}$$

Table 10 presents the proposed regression parameters and the associated standard deviations of the vector IMs when k_y is also considered in the models. It is seen that combination of PGV with I_a , PGA and k_y /PGA yields the most efficient vector models. From these vector models only PGV- I_a and PGV- k_y /PGA (shown in bold in Table 10)

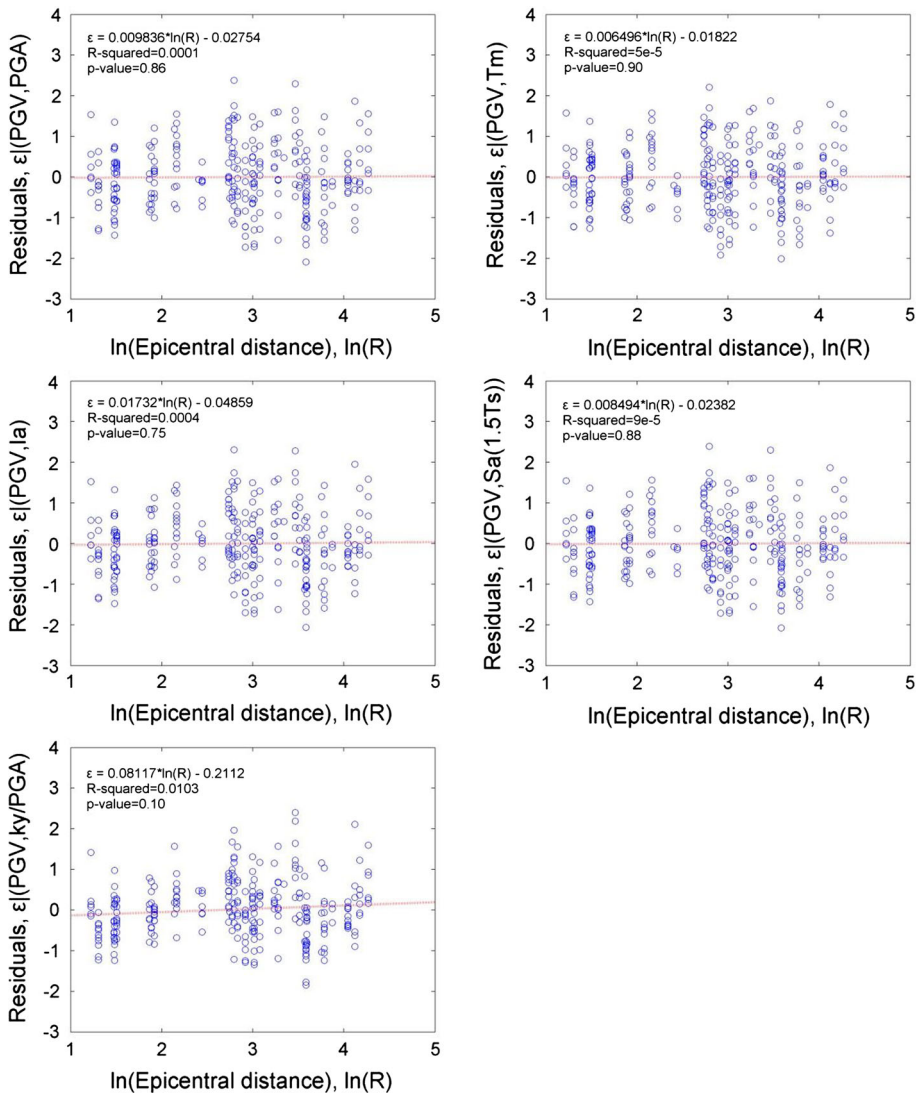


Fig. 16 Sufficiency of the studied vector IMs by examining the conditional statistical independence from epicentral distance

cover the sufficiency criterion and thus they are recommended for use. However, between the two vector models, PGV– k_y /PGA model is to be preferred taking into account the increased proficiency of k_y /PGA compared to I_a . As in the scalar IMs, a considerable increase in efficiency is observed when k_y term is added in the regression equation.

5.3 Suggested scalar and vector predictive models

Based on the optimally selected scalar and vector IMs, Eqs. 8–12 summarize the proposed scalar (Eqs. 8–10) and vector (Eqs. 11–12) predictive models for assessing the seismically induced slope displacement that are recommended for use in practice:

Table 10 Demand models and their associated efficiency for the different considered vector IMs when considering the k_y term in the regression equation

IM ₁	IM ₂	ln(a)	b	c	e	σ
PGV (cm/s)	k_y/PGA	−8.360	1.873	−5.964	−0.347	0.64
PGV (cm/s)	T_m (s)	−8.310	1.873	−5.964	−0.380	0.66
PGV (cm/s)	I_a (m/s)	−8.076	1.873	−5.964	0.200	0.61
PGV (cm/s)	PGA (g)	−7.671	1.873	−5.964	0.334	0.64
PGV (cm/s)	$S_a(1.5T_s)$ (g)	−7.912	1.873	−5.964	0.189	0.66

$$\ln(D) = -9.891 + 1.873 \cdot \ln(\text{PGV}) - 5.964 \cdot k_y + 0.285 \cdot M \pm \varepsilon \cdot 0.65 \quad (8)$$

$$\ln(D) = -2.965 + 2.127 \cdot \ln(\text{PGA}) - 6.583 \cdot k_y + 0.535 \cdot M \pm \varepsilon \cdot 0.72 \quad (9)$$

$$\ln(D) = -10.246 - 2.165 \cdot \ln(k_y/\text{PGA}) + 7.844 \cdot k_y + 0.654 \cdot M \pm \varepsilon \cdot 0.75 \quad (10)$$

$$\ln(D) = -8.076 + 1.873 \cdot \ln(\text{PGV}) + 0.200 \cdot \ln(I_a) - 5.964 \cdot k_y \pm \varepsilon \cdot 0.61 \quad (11)$$

$$\ln(D) = -8.360 + 1.873 \cdot \ln(\text{PGV}) - 0.347 \cdot \ln(k_y/\text{PGA}) - 5.964 \cdot k_y \pm \varepsilon \cdot 0.64 \quad (12)$$

where D is in m, PGA in g, PGV in cm/s and I_a in m/s.

As discussed previously, the free field ground surface intensity parameters (i.e. PGA, PGV, I_a) estimated through a seismic hazard analysis that account for site effects could be used in the above equations without any depth modification. Otherwise, one could estimate the IMs for soil conditions (e.g. at the depth of the sliding surface) given the corresponding IMs at the rock outcrop using the simplified expressions proposed in this study (see Sect. 4).

5.4 Example application

A typical application of the proposed scalar and vector regression models is presented to exemplify the proposed analytical expressions to assess the co-seismic slope displacement providing also a comparison with Newmark-type methods. A natural step-like slope is considered with a yield coefficient k_y equal to 0.1. The elastic fundamental period of the slide mass T_s is estimated as 0.2 s assuming a maximum depth of the sliding mass and an average V_s equal to 15 m and 300 m/s respectively.

The scenario earthquake is represented by a real ground motion derived from the SHARE database (Seismic Hazard Harmonization in Europe, www.share-eu.org) that is recorded on soil conditions (soil class C according to EC8) with moment magnitude $M_w = 6.93$ and epicentral distance $R = 30$ km. Table 11 presents the main characteristics of the recorded ground motion while Table 12 depicts the estimated ground motion intensity parameters that will be used for the given example application.

The median (or mean) and the median (or mean) $\pm 1 \sigma$ predictions for the proposed scalar and vector models (see Sect. 5.3) as well as the corresponding predictions of the empirical Newmark-type models applied in this study are presented in Table 13 for the given earthquake event and slope properties.

It is seen that the proposed models within the framework of this study predict consistent displacement for the considered earthquake scenario and slope properties. The estimated median values vary from 0.118 to 0.140 m, resulting at a maximum difference in the

Table 11 Characteristics of the selected scenario earthquake

Date	Earthquake name	M_w	R (km)	Preferred FS	Station name	$V_{s,30}$ (m/s)	Database code
18/10/1989	Loma Prieta, USA	6.93	30	Reverse-oblique	Gilroy array #2	302	NGA_766_H1

Table 12 Estimated ground motion intensity parameters of the given earthquake event

PGA (g)	PGV (cm/s)	T_m (s)	I_a (m/s)	Sa (1.5 T_s) (g)
0.363	32.87	0.526	1.197	0.715

Table 13 Seismic slope displacement predictions for the proposed scalar and vector models and the Newmark-type empirical methods for the given slope properties and earthquake event

	Seismic slope displacement (m)		
	Median (or mean)	Median (or mean) +1 σ	Median (or mean) -1 σ
<i>Scalar models</i>			
PGV-M (Eq. 8)	0.140	0.267	0.073
PGA-M (Eq. 9)	0.126	0.259	0.061
k_y /PGA-M (Eq. 10)	0.118	0.249	0.056
<i>Vector models</i>			
PGV- I_a (Eq. 11)	0.123	0.226	0.067
PGV- k_y /PGA (Eq. 12)	0.140	0.241	0.074
Newmark	0.088	–	–
Jibson (2007)	0.355	0.657	0.192
Rathje and Antonakos (2011)	0.148	0.240	0.091
Bray and Travarasrou (2007)	0.259	0.499	0.134

prediction on the order of 15 %. In particular, the scalar k_y /PGA-M model predicts the smallest displacement (0.118 m) while the largest one is predicted by both the scalar PGV-M and the vector PGV- k_y /PGA models. Such differences are not considered important taking also into account the considerable aleatory variability associated to both the characteristics of the slope and the ground motion intensity parameters.

As shown in the table, for the scalar predictive models the estimated median +1 σ and median -1 σ displacements are about two times and half the median value respectively. Considering that the vector models are shown to display smaller σ values, the estimated range of the median $\pm 1 \sigma$ displacements is even more converged for the proposed two-parameter vector models.

A comparison between the slope displacements estimated by the models recommended for use in this study and the corresponding displacements predicted by the empirical models is also performed (see Table 13). It is observed that Newmark analytical rigid block method predicts an average displacement that is 25–37 % smaller than the median displacements estimated by the proposed models, while the remaining simplified models

overpredict the corresponding displacements. In particular, Jibson (2007), Rathje and Antonakos (2011) and Bray and Travararou (2007) present 150–200, 6–25 and 85–120 % larger displacements respectively compared to the ones predicted by the herein proposed relationships. These findings that are generally in line with the observations presented in Sect. 4 indicate the significant uncertainties (both aleatory and epistemic) associated with the modeling assumptions as well as with the selection of the intensity parameters and slope properties in the different approaches highlighting the need for a probabilistic assessment of the seismically induced slope displacements.

6 Conclusions

The seismic performance of slopes is commonly evaluated by using a displacement based procedure which relates the earthquake induced slope displacement with some metric(s) of the seismic ground motion and the main geometrical and mechanical features of the slope.

Within the framework of this study, earthquake-induced slope displacements were calculated using an advanced numerical parametric analysis considering different slope geometries, material properties and input motions. The computed numerical displacements were first compared with some of the most widely used empirical Newmark-type displacement procedures, namely the conventional analytical Newmark rigid block model (Newmark 1965), Jibson (2007) rigid block model, Rathje and Antonakos (2011) decoupled sliding block model and Bray and Travararou (2007) coupled stick–slip sliding block model. Relatively good correlations were observed enhancing the reliability of the numerical analysis results. However, a large dispersion in the displacement estimation is shown. Generally, it is seen that the simplified empirical models displayed greater variability with respect to the numerical analysis compared to the analytical Newmark method.

Then, linear regression analyses were performed on the numerical analysis results to correlate the computed displacements with various IMs. Optimal scalar and two-parameter vector IMs were identified based on proficiency and sufficiency criteria. The correlation coefficient between the IMs was also considered an important factor for the selection of appropriate vector IMs. It has been shown that PGV, PGA and k_y/PGA are the optimal scalar IMs while $PGV-I_a$ and $PGV-k_y/PGA$ represent the best vector IMs. Based on these observations, both scalar and vector linear regression models were developed to assess the co-seismic slope displacement. It is observed that the standard deviation in the displacement prediction is reduced for the proposed vector models compared to the scalar ones. However, despite this increase in efficiency, the vector models introduce additional uncertainties associated with the estimation of the ground motion hazard for the vector of IMs. k_y term, which represents the overall resistance of the slope, is also incorporated in the regression equations considering its importance in slope displacement estimation. In addition, to eliminate bias associated to the dependence of the scalar models on the earthquake magnitude (and thus to cover the sufficiency criterion with respect to magnitude), a magnitude term is also added in the suggested scalar analytical expressions.

The developed displacement models can be used as predictive tools for assessing the performance of slopes within a deterministic or probabilistic framework for application at regional or local scales. A typical deterministic example, where the co-seismic permanent slope displacements were estimated using the proposed analytical expressions and the empirical Newmark-type methods, has been also presented. It has been shown that all proposed models predict consistent seismic slope displacements for the considered

earthquake scenario and slope properties. The comparison with the empirical approaches illustrated the large variability in the displacement prediction highlighting the superiority of the probabilistic over the deterministic approach in the evaluation of the seismically induced slope displacement (e.g. Rathje et al. 2014). Thus, future work should be devoted to the implementation of the proposed herein predictive models using a probabilistic approach which will account rigorously for the various sources of uncertainty involved (both aleatory and epistemic) in the assessment of the earthquake induced slope displacement.

References

- Ambraseys NN, Menu JM (1988) Earthquake-induced ground displacements. *J Earthq Eng* 16:985–1006
- Baker JW, Cornell CA (2006) Correlation of response spectral values of multicomponent ground motions. *Bull Seismol Soc Am* 96(1):215–227
- Bray JD (2007) Simplified seismic slope displacement procedures. In: Pitilakis KD (ed) *Earthquake geotechnical engineering*. Springer, Berlin
- Bray JD, Rathje ER (1998) Earthquake-induced displacements of solid-waste landfills. *J Geotech Geoenviron Eng ASCE* 124(3):242–253
- Bray JD, Travarasrou T (2007) Simplified procedure for estimating earthquake-induced deviatoric slope displacements. *J Geotech Geoenviron Eng ASCE* 133(4):381–392
- Cai Z, Barhurst RJ (1996) Deterministic sliding block methods for estimating seismic displacements of earth structures. *Soil Dyn Earthq Eng* 15:255–268
- Cundall PA, Hansteen H, Lacasse S, Selnes PB (1980). NESSI: soil structure interaction program for dynamic and static problems. Report 51508-9, December, Norwegian Geotechnical Institute
- Itasca Consulting Group (2011) Inc. FLAC (Fast Lagrangian Analysis of Continua), version 7.0. Itasca Consulting Group, Inc., Minneapolis
- Jibson RW (2007) Regression models for estimating co seismic landslide displacement. *Eng Geol* 91:209–218
- Jibson RW (2011) Methods for assessing the stability of slopes during earthquakes: a retrospective. *Eng Geol* 122(1–1):43–50
- Kwok AO, Stewart JP, Hashash YMA, Matasovic N, Pyke R, Wang Z, Yang Z (2007) Use of exact solutions of wave propagation problems to guide implementation of nonlinear seismic ground response analysis procedures. *J Geotech Geoenviron Eng* 133(11):1385–1398
- Lin JS, Whitman R (1986) Earthquake induced displacements of sliding blocks. *J Geotech Eng* 112(1):44–59
- Luco N, Cornell AC (2007) Structure-specific scalar intensity measures for near-source and ordinary earthquake ground motions. *Earthq Spectra* 23(2):357–392
- Lysmer J, Kuhlemeyer RL (1969) Finite dynamic model for infinite media. *J Eng Mech* 95(EM4):859–877
- Makdisi F, Seed H (1978) Simplified procedure for estimating dam and embankment earthquake induced deformations. *J Geotech Eng* 104(7):849–867
- Meehan CL, Vahedifard F (2013) Evaluation of simplified methods for predicting earthquake-induced slope displacements in earth dams and embankments. *Eng Geol* 152:180–193
- Mejia LH, Dawson EM (2006) Earthquake deconvolution for FLAC. In: *Proceedings of the 4th international FLAC symposium, Madrid, Spain*, pp 211–219
- Morales-Esteban A, Justo JL, Reyes J, Azañón JM, Durand P, Martínez-Álvarez F (2015) Stability analysis of a slope subject to real accelerograms by finite elements. Application to San Pedro cliff at the Alhambra in Granada. *Soil Dyn Earthq Eng* 69:28–45
- Newmark NM (1965) Effects of earthquakes on dams and embankments. *Geotechnique* 15(2):139–159
- Padgett JE, Nielson BG, DesRoches R (2008) Selection of optimal intensity measures in probabilistic seismic demand models of highway bridge portfolios. *Earthq Eng Struct Dyn* 37:711–725
- Rathje EM, Antonakos G (2011) A unified model for predicting earthquake-induced sliding displacements of rigid and flexible slopes. *Eng Geol* 122(1–2):51–60
- Rathje EM, Bray JD (2000) Nonlinear coupled seismic sliding analysis of earth structures. *J Geotech Geoenviron Eng ASCE* 126(11):1002–1014
- Rathje EM, Wang Y, Stafford P, Antonakos G, Saygili G (2014) Probabilistic assessment of the seismic performance of earth slopes. *Bull Earthq Eng* 12:1071–1090

- Sarma SK (1975) Stability analysis of embankments and slopes. *Geotechnique* 25(4):743–761
- Saygili G, Rathje EM (2008) Empirical predictive models for earthquake-induced sliding displacements of slopes. *J Geotech Geoenviron Eng ASCE* 134(6):790–803
- Shome N (1999) Probabilistic seismic demand analysis of nonlinear structures. Ph.D Thesis, Stanford University
- Strenk PM, Wartman J (2013) Influence of ground motion variability on seismic displacement uncertainty. In: Proceedings of the 18th international conference on soil mechanics and geotechnical engineering, Paris
- Travasariou T (2003) Optimal ground motion intensity measures for probabilistic assessment of seismic slope displacements. Ph.D. Dissertation, U.C. Berkeley
- Travasariou T, Bray JD (2003) Optimal ground motion intensity measures for assessment of seismic slope displacements. In: 2003 Pacific conference on earthquake engineering, Christchurch, New Zealand
- Watson-Lamprey J, Abrahamson N (2006) Selection of ground motion time series and limits on scaling. *Soil Dyn Earthq Eng* 26(5):477–482
- Yegian M, Marciano E, Ghahraman V (1991) Seismic risk analysis for earth dams. *J Geotech Eng* 117(1):18–34